BNL - 69514
CAP - 352-ATF-02C

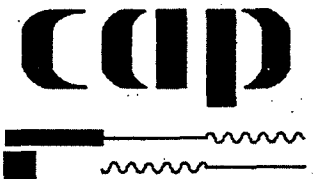

Primary Tests of Laser/e Beam Interaction In a Plasma Channel

I.V. Pogorelsky [a], I. Ben-Zvi [a], T. Hirose [b], V. Yakimenko [a], K. Kusche [a], P. Siddons [a], T. Kumita [b], Y. Kamiya [b], F. Zhou [c], A. Zigler [d], B. Greenberg [d], D. Kaganovich [d], I.V. Pavlishin [e], A. Diublov [e], N. Andreev [f], N. Bobrova [g] and P. Sasorov [g]

[a] *Accelerator Test Facility, Brookhaven National Laboratory, 820, Upton, NY 11973, USA*
[b] *Physics Department, Tokyo Metropolitan University, Japan*
[c] *University of California at Los Angeles, Los Angeles, CA 90024, USA*
[d] *Hebrew University, Jerusalem, Israel*
[e] *Optoel-Intex Co, St. Petersburg, Russia*
[f] *Inst. High Density Energy, Moscow, Russia*
[g] *Inst. Theoretical and Experimental Phys., Moscow, Russia*

October 2002

CENTER FOR ACCELERATOR PHYSICS

BROOKHAVEN NATIONAL LABORATORY
BROOKHAVEN SCIENCE ASSOCIATES

Under Contract No. DE-AC02-98CH10886 with the
UNITED STATES DEPARTMENT OF ENERGY

Submitted to "Workshop for Advanced Accelerator Concepts 2002", Oxnard, California, June 23-28, 2002.

Primary tests of laser/e-beam interaction in a plasma channel

I.V. Pogorelsky [a], I. Ben-Zvi [a], T. Hirose [b], V. Yakimenko [a], K. Kusche [a], P. Siddons [a], T. Kumita [b], Y. Kamiya [b], F. Zhou [c], A. Zigler [d], B. Greenberg [d], D. Kaganovich [d], I.V. Pavlishin [e], A. Diublov [e], N. Andreev [f], N. Bobrova [g] and P. Sasorov [g]

[a] *Accelerator Test Facility, Brookhaven National Laboratory, 820, Upton, NY 11973, USA*
[b] *Physics Department, Tokyo Metropolitan University, Japan*
[c] *University of California at Los Angeles, Los Angeles, CA 90024, USA*
[d] *Hebrew University, Jerusalem, Israel*
[e] *Optoel-Intex Co, St. Petersburg, Russia*
[f] *Inst. High Density Energy, Moscow, Russia*
[g] *Inst. Theoretical and Experimental Phys., Moscow, Russia*

Abstract. A high-energy CO_2 laser is channeled in a capillary discharge. Plasma dynamic simulations confirm occurrence of guiding conditions at the relatively low axial plasma density $1\div4\times10^{17}$ cm^{-3}. A relativistic electron beam transmitted through the capillary changes its properties depending upon the plasma density. We observe focusing, defocusing or steering of the e-beam. Counter-propagation of the electron and laser beams in the plasma channel results in generation of intense picosecond x-ray pulses.

1. INTRODUCTION

High-power laser guided in plasma channels is a prospective driver for the next-generation high-gradient electron accelerators where electrons pick up momentum from the laser photons moving collinear with the laser beam.

When the laser and electron beam motion is altered to counter-propagation, electrons lose energy generating intense x-ray pulses via Thomson scattering. This process can benefit from optical guiding as well allowing efficient use of relatively long laser pulses.

Preparing grounds for experimental investigation of both electron acceleration and x-ray generation, the BNL ATF, in collaboration with Hebrew University, Jerusalem, initiated in 1999 R&D on the e-beam compatible plasma channel suitable to guide mid-infrared ($\lambda\approx10$ μm) CO_2 laser radiation, which is one of the ATF's specialties. In 2000 this study became a part of the ongoing project "Development of Polarized Positron Source for Japan Linear Collider" [1] supported by the Japan-US collaboration grant in High Energy Physics.

Several problems are to be solved in order to put plasma channel technology to work for the ATF laser/e-beam interaction experiments. These include:

- Finding conditions for channeling intense CO_2 laser pulses. Note that only shorter wavelength ($\lambda\approx1$ μm) solid state lasers have been used in previous plasma channel demonstrations.

- Upgrade the status of the plasma channel technology from being a subject of study to a robust user-friendly applied tool.
- Integrate a plasma channel into an electron beamline.

Final solutions to these problems are still ahead. However, important steps have been taken already during the first plasma-guided laser/e-beam interaction tests at the ATF. The following tasks have been accomplished in the course of the experiment on Thomson scattering in a plasma channel conducted in March 2002:

- We established conditions for producing cylindrically profiled plasma density on the scale of ~10^{17} cm^{-3} and demonstrated channeling of an intense CO_2 laser beam.
- Capillary discharge setup has been integrated into a laser/e-beam and is proved to be compatible with the electron linac high-vacuum conditions and high-power laser optics.
- Intense Thomson x-rays have been observed upon counter-propagation of the electron and laser beams through a plasma channel.
- We observed effects of e-beam manipulation by plasma of the capillary discharge that opens new potentials for e-beam focusing, steering and electron/laser synchronization.

2. MOTIVATION

The concept of using a plasma channel for next generation laser wakefield accelerators is well known. In this case the channel shall allow an increase of the particle energy gain by extending acceleration from a characteristic triple Rayleigh distance $\pi z_L = \pi^2 w_L^2 / \lambda$, which is of the order of millimeters, up to the dephasing length $L_{ph} = \lambda_p^3 / \lambda^2$, which is typically several centimeters long. In the equations above w_L is the radius of the laser focus and λ_p is the plasma wavelength. In addition, a properly profiled plasma channel allows further increase of the dephasing length [2].

The idea of using a laser channel to enhance x-ray production in Thomson scattering [3,4] is less familiar to the scientific community. In the present Section we revisit this subject that became the first motivation for the plasma channel study initiated at the ATF.

The ATF Thomson scattering experiment is based on a combination of a photocathode RF linac and a picosecond CO_2 laser in the exact 180^0 counter-propagation configuration. To compare with other previously demonstrated and proposed Thomson sources driven by solid state lasers, the CO_2 laser driver offers advantages reviewed in [4,5]. For example, a CO_2 laser beam carries 10 times more photons than a solid state laser of the same power. This implies a proportionally higher x-ray production.

The first ATF experiment conducted in 1999 demonstrated the record x-ray yield in relativistic Thomson scattering [4,6]. In 2001 the experiment has been repeated with more energetic CO_2 laser and demonstrated nearly proportionally high x-ray yield. This later result has not been published and we briefly review it below.

The 2001 experiment uses the same set-up as is shown in Fig.1 of Ref.[4]. The 5 J, 180 ps (FWHM) CO_2 laser pulses are focused with a parabolic mirror in counter-propagation with the 60 MeV, 0.5 nC, 3.5 ps (FWHM) e-beam. A small hole in the mirror transmits the backscattered x-rays and the spent electron beam.

The Thomson scattered x-rays are detected by a calibrated Si diode. On the way to the detector, the x-ray beam passes a 250 μm thick Be window and the 20 cm distance in the air. The electron beam is separated from the x-rays by a bending dipole magnet.

When the laser and electron beams are aligned and synchronized, we observe Thomson x-ray signal that corresponds to 1.4×10^{11} eV of the integral energy deposition on the detector. Based on CAIN simulation, this number is equivalent to 2.5×10^{7} photons/pulse.

Fig. 1 shows the simulated x-ray energy spectrum at the position of the detector. Low energy x-rays are attenuated in the Be window and air. Thus, just 15% of the total scattered photons reach the Si detector. Based on this, we calculate 1.7×10^{8} photons/pulse produced at the interaction point. Since pulse duration of the x-ray signal is equal to the electron bunch length (3.5 ps), peak photon density is estimated at 5×10^{19} photons/second.

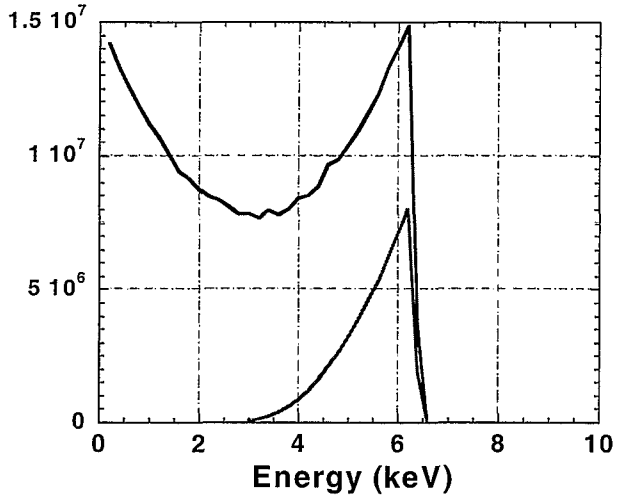

FIGURE 1: Simulated X-ray energy spectra. The upper line shows the spectrum of all photons generated at the interaction point, while the lower line shows photons that reach the detector.

The x-ray yield scales as

$$N_X \propto E_L Q\lambda / w_L^2 , \qquad (1)$$

where E_L and Q are correspondingly portions of the laser pulse energy and the electron bunch charge participating in the interaction. Simulations show that a great fraction of this yield is observed from the double Rayleigh length $2z_L=2\pi w_L^2/\lambda$, which is of the order of millimeters. Thus, a significant fraction of the 180 ps CO_2 pulse is wasted.

Presently the ATF CO_2 laser pulse duration is limited by a narrow bandwidth of the laser amplifier. The ongoing ATF laser upgrade includes installing a high-pressure broad-bandwidth amplifier that allows shortening the pulse duration to ~1 ps leading to significant increase of the x-ray yield in the Thomson scattering experiment.

With the CO_2 laser, electrons reach a relativistic quiver motion at the laser intensity of 10^{16} W/cm^2 to compare with 10^{18} W/cm^2 for the 1-μm laser. We can approach this intensity with the 1 TW CO_2 laser and expect to observe strong harmonics above the fundamental radiation [7].

Characterization of the nonlinear Thomson scattering effect presents high scientific interest. However, it is simultaneously a fundamental limitation on the way to increase spectral brightness of the Thomson x-ray source. Indeed, the expression for the short-wavelength edge in Thomson scattering

$$\lambda_x = \frac{\lambda\left(1+a^2/2\right)}{4\gamma^2} \tag{2}$$

shows the dependence upon the laser strength parameter

$$a = eE/mc = 0.85\times10^{-9}\,\lambda[\mu m]I^{1/2}\left[W/cm^2\right]. \tag{3}$$

This parameter varies in time and due to spatial intensity distribution in the focused laser beam that results in the considerable smearing of the integral x-ray spectrum. Finally, we arrive to a situation when the x-ray bandwidth becomes intensity dominated; that means that the increase in the laser intensity beyond a=1 does not improve the spectral brightness. This constraint can be alleviated only when we deliver the laser energy in a relatively long pulse maintaining a<<1. Such a long laser pulse can be used efficiently only if the laser-electron interaction region is confined in the extended plasma channel.

3. PLASMA CHANNEL FOR CO_2 LASER

3.1 Status of Capillary Discharge Technology

In choosing a laser guiding method applicable to the ATF Thomson scattering experiment, we apply the following selection rules:

- The channel shall not obscure the produced x-ray cone. This eliminates the use of a narrow micro-capillary.
- The plasma density needs to be much lower than 10^{19} cm^{-3} that is the critical density for the 10-μm beam. This requirement practically rules out methods based on optical breakdown in gas.

We select the capillary discharge scheme that allows controlling the plasma density [8]. It has been demonstrated previously that the laser beam can be confined in the plasma core ~10 times smaller than the physical diameter of the discharge tube. This allows interaction between the laser and electron beam and extraction of the Thomson scattered x-rays without obstruction by the tube walls.

Until now, all the plasma channel experiments have been performed using picosecond solid state lasers. However, the condition for plasma channeling

$$\Delta n_e\left[cm^{-3}\right]\cong 10^{20}/w_L^2\left[\mu m\right], \tag{4}$$

where Δn_e is the radial increase in the electron plasma density from r=0 to r=w_L, is not sensitive to the laser wavelength.

The method of the plasma channel formation via electric discharge in evacuated dielectric tubes has been introduced and perfected by researchers from Hebrew University, Jerusalem (A. Zigler et. al.) [2, 8-10]. They demonstrated the best performance from a double-stage capillary of several hundred micron bore size made of a plastic material such as polyethylene or polypropylene. High-voltage discharge in a short "ignition" capillary segment generates plasma by the inner wall ablation injecting it into the main several centimeters long capillary. When the ignition plasma fills the capillary the main storage capacitor discharges producing further ablation. Since the basic chemical composition of the capillary is CH_2, the plasma consists of protons and highly stripped carbon ions. The peak temperature of the discharge is typically 4 eV.

In the course of the main electrical discharge, there is an extended period of time (hundreds of nanoseconds) during which the pressure is uniform across the channel but the current density and plasma temperature have maxima along the axis. This results in the plasma density minimum at the axis. Under these conditions, the 2-TW λ=0.8 μm laser beam has been channeled over 22 z_L with the matched beam diameter 35 μm [9]. In another experiment the laser has been transported over the 75 z_L distance even through a curved capillary [10].

The on-axis plasma density obtained in the previous capillary discharge experiments is $(3\div5)\times10^{18}$ cm^{-3}. That is in proximity to the critical electron plasma density n_{cr}=10^{19} cm^{-3} for the λ=10 μm radiation to compare with the 10^{21} cm^{-3} for λ=1 μm.

CO_2 laser pulse propagating in subcritical plasma will lose its energy due to inverse bremsstrahlung over a distance

$$L_D=\frac{\omega_0^2}{\omega_p^2}\frac{c}{\nu_{ei}}, \tag{5}$$

where ω_0 is the laser angular frequency and ω_p is the plasma frequency; $\nu_{ei}=N_i v\sigma$ is the electron-ion collision frequency, v is the electron velocity and σ is the cross section for momentum transfer collisions.

Understanding that both ω_p^2 and ν_{ei} are ultimately proportional to the electron plasma density n_e we see that L_D scales with n_e^{-2}. To calculate L_D at n_e<n_{cr} we need an estimate for ν_{ei}, which is a function of the atomic content, degree of ionization, electron and ion temperature. For typical conditions of the hydrogen plasma, $v\sigma\approx1.6\times10^{-7}$ $cm^{-3}s^{-1}$ and $L_D\approx2$ cm @ n_e=10^{18} cm^{-3}.

Thus, in order to adapt the plasma channel technique to a CO_2 laser, the plasma density needs to be downscaled by 1-2 orders of magnitude to compare with that previously demonstrated in capillary discharges. Fortunately, the plasma density is a strong function of the discharge current and capillary tube inner radius, $n_e\sim IR_{cap}^{-2}$ [8]. Following this algorithm, the increase of the capillary radius to 1 mm shall make the plasma density range of n_e=$10^{17}\div10^{18}$ cm^{-3} accessible.

3.2 Simulations of CO_2 Laser Channeling in Capillary Discharge

Simulations of channeling of the CO_2 laser pulses in a moderately dense plasma have been performed by solving a set of Maxwell and hydrodynamic equations for plasma electrons and ions. Plasma is considered fully ionized. Together with the preset parabolic plasma profile presumably produced in the capillary discharge, the model considered plasma response to the relatively long laser pulse that leads to the radial ponderomotive plasma expulsion and ponderomotive self-focusing of the laser beam.

In the numerical modeling we assume the following CO_2 laser parameters: temporal and radial Gaussian profile, pulse duration 180 ps, laser focus radius at the entrance to the channel w_0=45 μm, z_L=1.27 mm.

The space distribution of the background ion density in the channel is homogeneous along the axis with the parabolic increase in the radial direction

$$n_e = n_{e0}(r=0)\left[1+\frac{r^2}{R_{ch}^2}\right]. \qquad (7)$$

The channel radius is matched to the plasma density and laser focal radius by the condition $R_{ch} = k_{p0} w_L^2$, where $k_{po} = \omega_{p0}/c$. In the linear regime, the matched laser beam propagates along the channel without oscillations and distortions [11].

To investigate dynamics of laser pulse channeling we modeled the laser pulse propagation at the background plasma densities on the axis between n_e=(1÷4)×10^{17} cm^{-3} with the characteristic radius of the channel R_{ch}=127÷255 μm. The increase in the background plasma density leads to more pronounced ponderomotive modulation of the channel density and as a consequence to the nonlinear modulation of the laser intensity as is shown in Fig.2.

The laser channeling simulations show the importance of matching the laser beam focus to the plasma channel size. For example, broadening the channel by a factor of two for the same laser beam size results in strong periodical oscillations of the laser envelope radius between 130÷250 μm. In order to avoid this situation, it is important to understand the plasma profiles produced via capillary discharge and factors that affect these profiles.

Spatial and time dependence of plasma electron density and temperature in the electrical capillary discharge has been evaluated by one-dimensional MHD simulation, which is valid since the length of the capillary is much larger than its diameter.

The following dissipative processes are taken into account: electron thermal conductivity, Joule heating, Nernst and Ettinghausen effects, the radiation losses and ion viscosity. To calculate the degree of ionization we assume that the conditions for the local thermodynamic equilibrium are satisfied. The plasma-wall interaction is modeled by considering the material of the wall as a cold neutral gas with atomic number Z=7, average atomic weight A=14, and initial density ρ_0 = 1 g/cm^3. The capillary plasma is driven by a current pulse approximated by the empirical formula $I(t)=I_0\sin(\pi t/150\text{ns})\exp(-t/375\text{ns})$, where I_0=486 A.

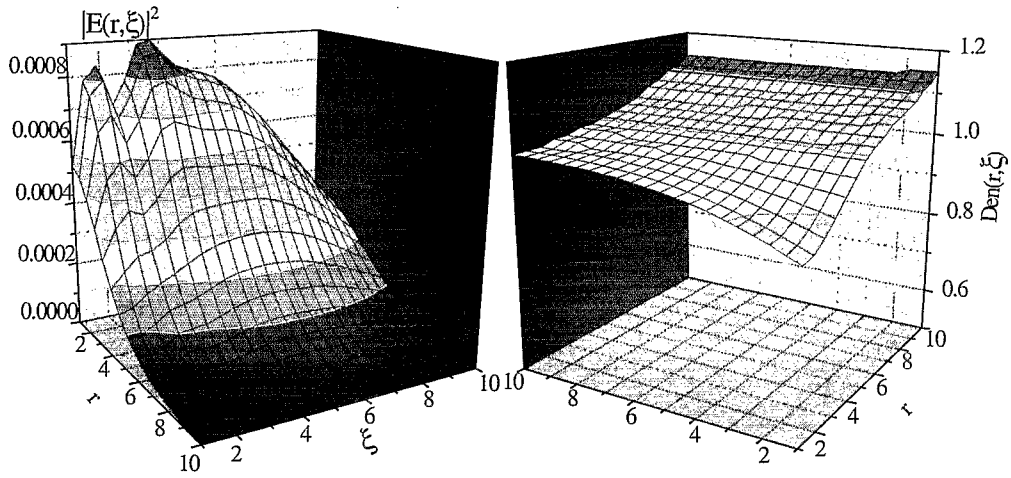

FIGURE 2: Laser and plasma channel profiles for the following initial conditions: laser pulse duration 180 ps peak power 0.6 GW, plasma density at the axis 4×10^{17} cm^{-3} ,.

The MHD simulation results shown in Fig.3 predict obtaining plasma channel conditions (radial increase of the plasma density) in the exact range $n_{eo}=(1\div4)\times10^{17}$ cm^{-3} as has been used in above simulations of the laser pulse propagation. Fitting parabolic approximations to the simulated plasma profiles we obtain $R_{ch}=425\div450$ μm and the practically achievable matched $w_L = 55\div75$ μm.

The experimental results reported in the next Section indicate that the capillary discharge efficiently confines the ATF CO_2 laser beam.

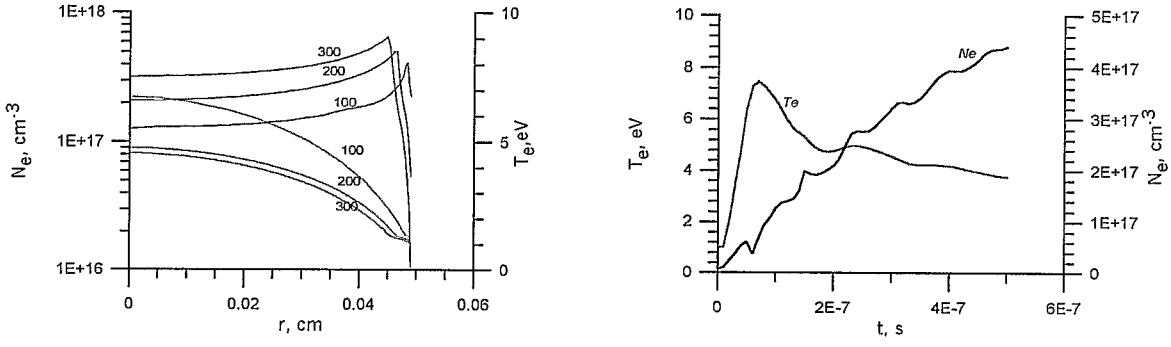

FIGURE 3. MHD simulations of the plasma channel formation in the capillary discharge

3.3 Capillary Discharge Setup

Establishing a relatively low-density plasma channel is just one in a series of tasks to adopt the capillary discharge technology for the ATF user's experiments. Among other requirements we considered:

- Ease and sufficiency of the capillary manipulation inside the vacuum interaction cell.

- Reproducible, low jitter, low inductance discharge based on high duty, reliable circuitry and vacuum compatible components.
- Compact, vacuum compatible overall design.

To ensure that our requirements are incorporated into the state-of-the-art device, we employed a commercial company OPTOEL Co, St. Petersburg, Russia. The company designed, assembled, and tested the interaction cell that incorporates the capillary discharge device.

The interaction cell designed as a triple-section assembly (see Fig.4a) has been built at MDC Co. The end sections incorporate parabolic mirrors (Power Optics Inc.) with manipulators (Thermionics and New Focus). The capillary setup is incorporated into the central section shown schematically in Fig.4b.

A custom capillary holder is mounted on a combination of translation and tilt manipulators (Thermionics and MDC). Standard electrical feedthroughs transmit high-voltage potentials to internal electrical components as shown in Fig.5.

A polypropylene capillary tube of the 1 mm inner diameter and 18 mm length has been positioned inside a vacuum chamber (~10^{-5} torr). Up to 14 kV pulsed voltage is applied to the capillary electrodes. The 200-ps, 100-mJ CO_2 laser pulse was focused at the entrance of the capillary. The output laser beam has been imaged with 7X magnification to the Electrophysics pyroelectric video-camera. Intensity profiles are grabbed with the Spiricon laser beam analyzer.

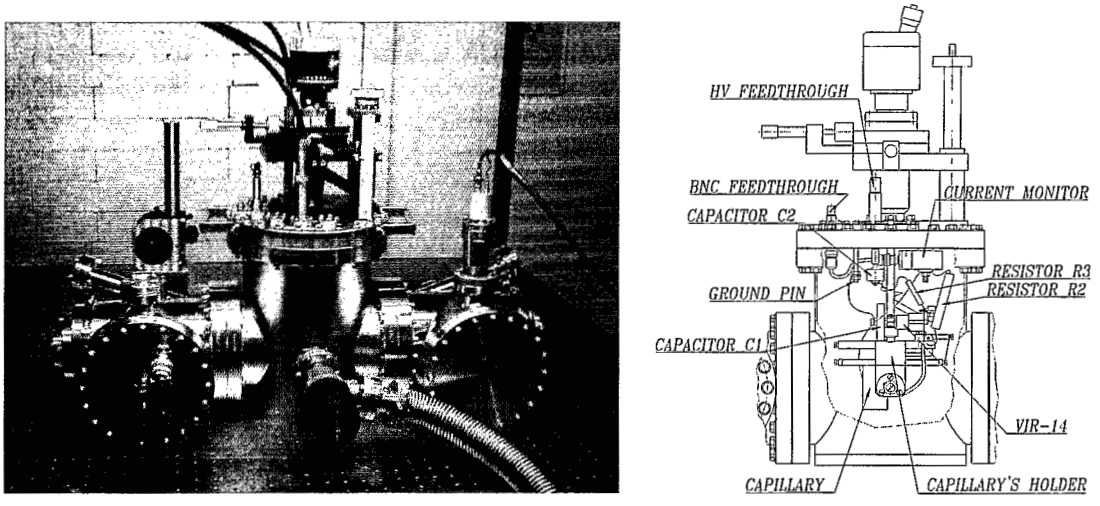

(a) (b)

FIGURE 4. a) View of the interaction cell; b) Diagram of the central section containing the capillary

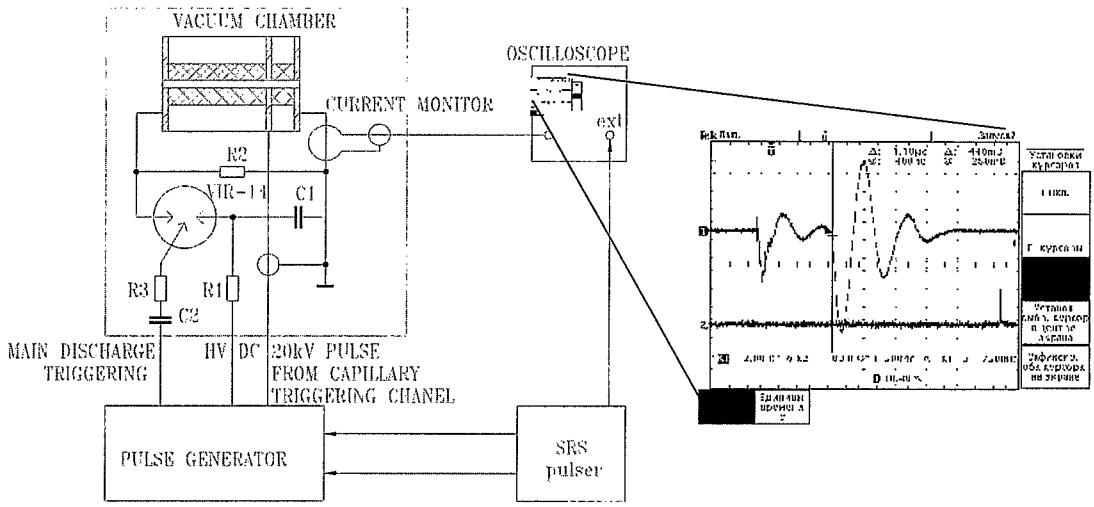

FIGURE 5. Principle diagram of the capillary discharge circuit with the double discharge current trace on the insert

Intensity distributions shown in Fig. 6a and 6b are obtained in "free space" (capillary retracted). Fig. 6a is taken at the focal point. Fig. 6b is taken at 18 mm distance downstream from the focus. Note that in order to stay within a linear response of the camera and the frame-grabber, images 6a and 6b are obtained with different attenuation. This permits measurement of the beam size that, as we see, expands approximately 6 times in diameter between the observation points spaced by ~ 6 z_L. The best channeling condition is obtained at the 12-14 kV voltage applied to the capillary, peak current ~400 A, and the laser pulse delayed by ~120 ns relative to the first current peak.

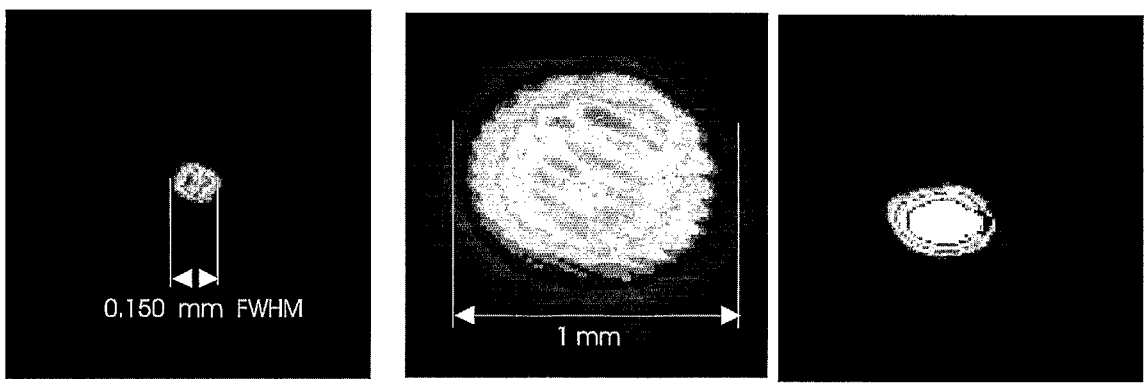

FIGURE 6. CO_2 laser beam profiles:
a) at the focal point; b) 18 mm downstream from the focus in the free space propagation; c) at the exit of the 18 mm long plasma discharge with the capillary entrance placed at the focal point (no attenuation adjustment between b) and c)).

The result shown in Fig. 6 appears to be the first experimental evidence of the 10-μm laser beam guiding in a plasma channel. Our observations, being of a special importance

for the CO_2 laser applications, simultaneously provide more general confirmation of establishing a plasma channel in the range of $10^{17} \div 10^{18} cm^{-3}$. These conditions are of interest for such important application of guided laser beams (including solid state lasers as well) as laser wakefield acceleration.

4. TEST OF RELATIVISTIC THOMSON SCATTERING IN A PLASMA CHANNEL

Location and configuration for this first test of the laser/e-beam interaction in a plasma channel is very similar to the previous ATF Thomson scattering experiments. A principle diagram of the experiment is shown in Fig.7.

Our observations based on the run conducted in March 2002 can be summarized as follows:

- ~80% of the e-beam charge transmission through the capillary.
- The x-ray bremsstrahlung background is sufficiently low to allow clean measurement of the Thomson effect.
- Variety of e-beam manipulation effects upon transmission through the plasma channel including: focusing, defocusing and steering.
- The x-ray yield is still at the level of our previous run with no observed enhancement due to a channel over the free-space interaction.

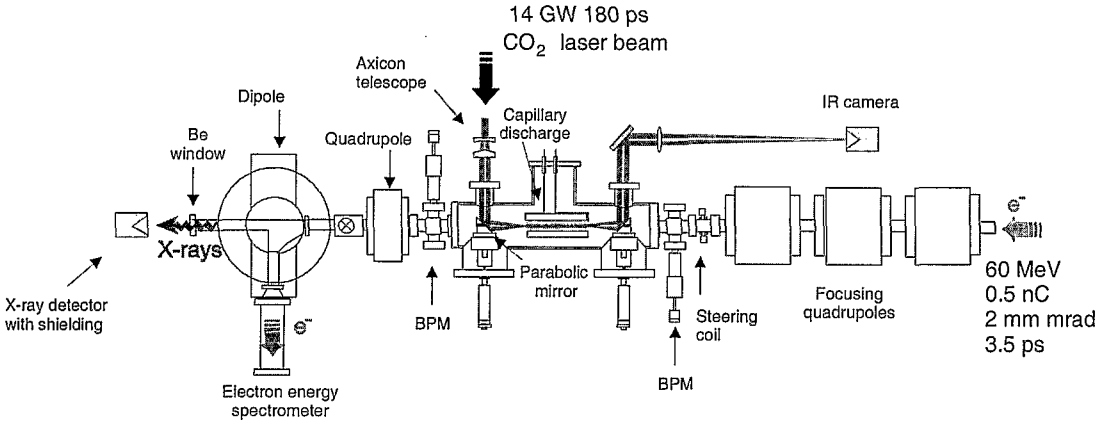

FIGURE 7. Principle diagram of the Thomson scattering experiment in a plasma channel.

The last of the aforementioned observations can be attributed to the bent e-beam trajectory due to a stray dipole field and degraded laser channeling during the run. The experiment will be repeated after these problems are fixed.

The effects of the e-beam manipulation by the plasma channel have been revealed by observing the beam profile variations on the phosphor screen placed under the 90° bending dipole that serves as an electron spectrometer. A variety of the observed effects can be attributed to the fact that the capillary double discharge provides several sources of cylindrically profiled plasma: 3 mm long trigger electric discharge, 18 mm long main electric discharge, laser optical breakdown, plus combinations of these plasma sources.

This enables a spectrum of plasma conditions: from overdense to underdense, variable longitudinal thickness and radial profile.

It is well known that, due to charge compensation in plasma, the focusing self-magnetic field of the relativistic bunch is not cancelled any more by the Coulomb repulsion. For the overdense plasma regime, when the electron density in the bunch is much smaller than the ambient plasma density, $n_b << n_e$, the focusing force can reach [12]

$$F_r / r \approx 2\pi n_b e^2 \approx 3\times 10^{-9} n_b [G/cm]. \quad (8)$$

For the ATF conditions, $n_b = N_b/(2\pi)^{3/2}\sigma_r^2\sigma_z \approx 10^{14}$ cm^{-3} and the focusing force approaches 3×10^5 G/cm that exceeds the strength of conventional quadrupole magnets. More accurate estimates require taking into account partial compensation of the self-induced magnetic field by the return current in plasma that becomes important when the electron beam size is comparable or greater than the plasma skin depth, i.e., $k_p\sigma_r \geq 1$.

For the future runs of the guided Thomson scattering experiment, we plan more systematic study of plasma lens effects implementing additional beam profile monitors after the capillary.

5. CONCLUSIONS

The following steps has been made on the way to put plasma channel technology in service for ATF user's experiments:

- Conditions for producing cylindrically profiled plasma density on the scale of ~10^{17} cm^{-3} have been established and intense CO_2 laser beam channeling is demonstrated.
- Capillary discharge setup has been integrated into a laser/e-beam interaction cell and is proved to be compatible with the electron linac high-vacuum conditions and high-power laser optics.
- The experiment on guided Thomson scattering has been installed in one of the ATF beamlines. Intense Thomson x-rays have been observed upon simultaneous transmission of the electron and laser beams through a plasma channel.
- We observed effects of e-beam manipulation by plasma of the capillary discharge that opens new potentials for e-beam focusing, steering and electron/laser synchronization.
- The reported experimental demonstration of a plasma channel in the range of 10^{17}cm^{-3} is of interest for such essential application of guided laser beams (including solid state lasers as well) as laser wakefield acceleration (LWFA). We will continue this search towards 10^{16}cm^{-3}. As soon as the ATF laser achieves the picosecond pulse duration we will be in position to run LWFA experiment just by reversing the laser propagation.

ACKNOWLEDGMENTS

Authors thank J. Skaritka and M. Woodle for engineering help. This study is supported by the U.S. Dept. of Energy under the Contract DE-AC02-98CH10886, Japan-US and Japan-Israel Cooperative Grants in High Energy Physics.

REFERENCES

1. Tsunemi, A., Endo, A., Washio, M., Hirose, T., Kurihara, Y., Omori, T., and Urakawa, T., *Proc. Int. Conf. Lasers'97*, December 15-19, 1997, New Orleans, LA, STS Press, McLean, VA, 839-844 (1998)
2. Kaganovich, D., Sasorov, P., Cohen, C., and *Appl. Phys. Rev. Lett.* **75**, 772-774 (1999)
3. Pogorelsky, I.V., Ben-Zvi, I., Wang, X.J., and Hirose, T., *Nucl. Instrum. & Methods in Phys. Res. A* **455**, 176-180 (2000)
4. Pogorelsky, I.V., Ben-Zvi, I., Hirose, T., Kashiwagi, S., Kusche, K., Kumita, T., Omori, T., Yakimenko, V., Yokoya, K., Urakawa, J., and Washio, M., *Proc. Adv. Accel. Workshop,* June 10-16, 2000, Santa Fe, NM, *AIP Conf. Proc.* **569**, 571-582 (2001)
5. Pogorelsky, I.V., *Nucl. Instrum. & Methods in Phys. Res. A* **411**, 172-187 (1998)
6. Pogorelsky, I.V., Ben-Zvi, I., Hirose, T., Kashiwagi, S., Yakimenko, V., Kusche, K., Siddons, P., Skaritka, J., Kumita, T., Tsunemi, A., Omori, T., Urakawa, J., Washio, M., Yokoya, K., Okugi, T., Liu, Y., He, P., and Cline, D., *Phys. Rev. ST-AB* **3**, 090702 (2000)
7. Pogorelsky, I.V., Ben-Zvi, I., Kusche, K., Siddons, P., Yakimenko, V., Hirose, T., Kumita, T., Kamiya, Y., Omori, T., Urakawa, J., Yokoya, K., Kashiwagi, S., Washio, M., Zigler, A., Greenberg, B., Kaganovich, D., Pavlichin, I.V., Meshkovsky I.K., Zhou, F., and Cline, D., *Proc. Int. Conf. Lasers'2001*, December 3-7, 2001, Tucson, AZ, STS Press, McLean, VA, 28-33 (2002)
8. Kaganovich, D., Sasorov, P.V., Zigler, A., Burris, R., Ehrlich, Y., *Appl. Phys. Lett.* **71**, 2925-2927 (1997)
9. Kaganovich, D., Ting, A., Moore, C.I., Zigler, A., Burris, H.R., Ehrlich, Y., Hubbard, R., and Sprangle, P., *Phys. Rev. E* **59**, R4769-R4772 (1999)
10. Ehrlich, Y., Cohen, C., Kaganovich, D., Zigler, A., Hubbard, R.F., Sprangle, P., and Esarey, E., *J. Opt. Soc. Am. B* **15**, 2416-2423 (1998)
11. Esarey, E., Krall, J., and Sprangle, P., *Phys. Rev. Lett.* **72**, 2887 (1994)
12. Su, J.J., Katsouleas, T., Dawson, M., and Fedele, R., *Phys. Rev. A* **41**, 3321-3331 (1990)